Title

A Sensitive Ultrahigh-Performance Liquid Chromatography/Tandem Mass Spectrometry Method for the Simultaneous Analysis of Phytocannabinoids and Endocannabinoids in Plasma and Brain.

Journal

Cannabis and Cannabinoid Research, 9(1)

Authors

Ahmed, Faizy

Torrens Miears, Alexa

Mahler, Stephen

et al.

Publication Date

2024-02-01

DOI

10.1089/can.2022.0216

Peer reviewed

Cannabis and Cannabinoid Research
Volume 9, Number 1, 2024

DOI: 10.1089/can.2022.0216

ORIGINAL RESEARCH

A Sensitive Ultrahigh-Performance Liquid Chromatography/Tandem Mass Spectrometry Method for the Simultaneous Analysis of Phytocannabinoids and Endocannabinoids in Plasma and Brain

Faizy Ahmed,[1,*] Alexa Torrens,[1] Stephen V. Mahler,[2] Francesca Ferlenghi,[3] Marilyn A. Huestis,[4] and Daniele Piomelli[1,5,6]

Abstract

Introduction: Δ^9-tetrahydrocannabinol (THC) and cannabidiol (CBD) are major chemical constituents of cannabis, which may interact either directly or indirectly with the endocannabinoid and endocannabinoid-like ("paracannabinoid") systems, two lipid-based signaling complexes that play important roles in physiology. Legislative changes emphasize the need to understand how THC and CBD might impact endocannabinoid and paracannabinoid signaling, and to develop analytical approaches to study such impact. In this study, we describe a sensitive and accurate method for the simultaneous quantification of THC, its main oxidative metabolites [11-hydroxy-Δ^9-THC (11-OH-THC) and 11-nor-9-carboxy-Δ^9-THC (11-COOH-THC)], CBD, and a representative set of endocannabinoid [anandamide and 2-arachidonoyl-*sn*-glycerol (2-AG)] and paracannabinoid [palmitoylethanolamide (PEA) and oleoylethanolamide (OEA)] compounds. Analyte separation relies on the temperature-dependent shape selectivity properties of polymerically bonded C18 stationary phases.

Materials and Methods: Analytes are extracted from tissues using acetonitrile precipitation followed by phospholipid removal. The ultrahigh-performance liquid chromatography/tandem mass spectrometry protocol utilizes a commercially available C18 polymeric-bonded phase column and a simple gradient elution system.

Results: Ten-point calibration curves show excellent linearity ($R^2 > 0.99$) over a wide range of analyte concentrations (0.02—500 ng/mL). Lowest limits of quantification are 0.05 ng/mL for anandamide, 0.1 ng/mL for 11-OH-THC and OEA, 0.2 ng/mL for THC and CBD, 0.5 ng/mL for 11-COOH-THC, 1.0 ng/mL for 2-AG, and 2.0 ng/mL for PEA. The lowest limits of detection are 0.02 ng/mL for anandamide, 0.05 ng/mL for 11-OH-THC and OEA, 0.1 ng/mL for THC and CBD, 0.2 ng/mL for 11-COOH-THC, 0.5 ng/mL for 2-AG, and 1.0 ng/mL for PEA.

Conclusions: An application of the method is presented, which showed that phytocannabinoid administration elevates endocannabinoid levels in plasma and brain of adolescent male and female mice.

Keywords: Δ^9-tetrahydrocannabinol; 2-arachidonoyl-*sn*-glycerol; anandamide; cannabidiol; endocannabinoid; shape selectivity; ultrahigh-performance liquid chromatography/tandem mass spectrometry

Introduction

The endocannabinoid system comprises two lipid-derived messengers, anandamide and 2-arachidonoyl-*sn*-glycerol (2-AG), which are endogenous agonists of the cannabinoid receptors, the same receptors that are directly or indirectly targeted by the cannabis-derived phytocannabinoids, Δ^9-tetrahydrocannabinol (THC) and cannabidiol (CBD).[1] Anandamide and 2-AG share biogenetic and degradative pathways with another group of lipid substances that do not activate

Departments of [1]Anatomy and Neurobiology, and [2]Neurobiology and Behavior, University of California, Irvine, California, USA.
[3]Dipartimento di Scienze degli Alimenti e del Farmaco, Università degli Studi di Parma, Parma, Italy.
[4]Institute of Emerging Health Professions, Thomas Jefferson University, Philadelphia, Pennsylvania, USA.
Departments of [5]Biological Chemistry, and [6]Pharmaceutical Sciences, University of California, Irvine, California, USA.

*Address correspondence to: Faizy Ahmed, PhD, Department of Anatomy and Neurobiology, University of California, 837 Health Sciences Road, Room 3107, Irvine, CA 92967, USA, E-mail: fahmed@uci.edu

Analyte	Structure
11-OH-THC	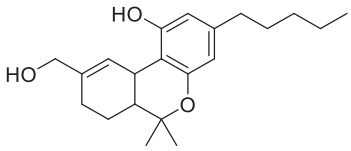
11-COOH-THC	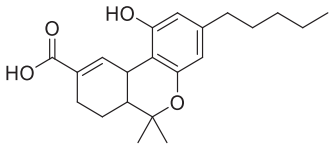
CBD	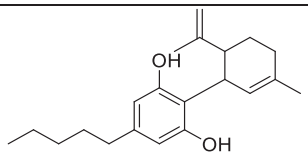
THC	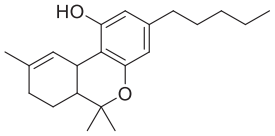
Anandamide	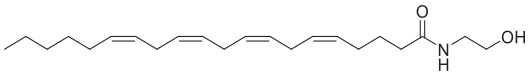
2-AG	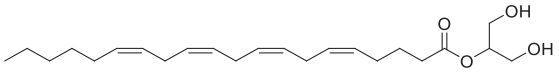
1-AG	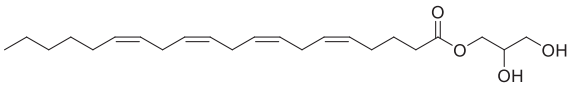
VEA	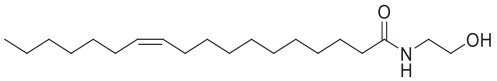
OEA	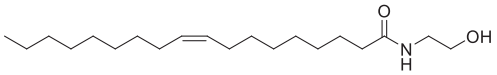
PEA	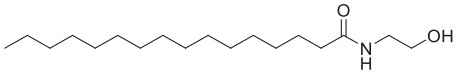

FIG. 1. Chemical structures of target analytes in order of elution from the LC column. 11-COOH-THC, 11-nor-9-carboxy-Δ^9-THC; 11-OH-THC, 11-hydroxy-Δ^9-THC; 2-AG, 2-arachidonoyl-*sn*-glycerol; CBD, cannabidiol; LC, liquid chromatography; OEA, oleoylethanolamide; PEA, palmitoylethanolamide; THC, Δ^9-tetrahydrocannabinol; VEA, vaccenoylethanolamide.

cannabinoid receptors but can functionally synergize or antagonize endocannabinoid activity by engaging various ligand-activated transcription factors and G protein-coupled receptors.[1–5] These endocannabinoid-like messengers (referred to here as "paracannabinoids") include fatty acyl ethanolamides such as palmitoylethanolamide (PEA) and oleoylethanolamide (OEA) as well as fatty acyl glycerol esters such as 2-oleoyl-*sn*-glycerol.[1]

Evidence from both animal and human studies suggests that THC and CBD may influence endocannabinoid and paracannabinoid signaling in significant ways.[6–9] Understanding this interaction and its consequences for human health is important at a time when medicinal and nonmedicinal cannabis use is becoming increasingly accepted.[10–12]

To support studies on this important topic, we developed a sensitive ultrahigh-performance liquid chromatography/tandem mass spectrometry (UHPLC-MS/MS) method to simultaneously quantify prominent phytocannabinoids [CBD, THC, and its two main oxidative metabolites, 11-hydroxy-Δ^9-THC (11-OH-THC) and 11-nor-9-carboxy-Δ^9-THC (11-COOH-THC)], endocannabinoids (anandamide, 2-AG), and paracannabinoids [PEA, OEA, along with the naturally occurring OEA analogue vaccenoylethanolamide (VEA)] in biological samples (see Fig. 1 for chemical structures). The method relies on the temperature-dependent shape selectivity properties of polymerically bonded C18 stationary phase and its advantages include sensitivity, speed, and low cost. An application to plasma and brain from adolescent male and female mice is presented.

Materials and Methods

Solvents and chemicals

THC, 11-OH-THC, 11-COOH-THC, CBD, anandamide, 2-AG, OEA, PEA, and their corresponding [^{2}H]-containing derivatives were obtained from Sigma-Aldrich (St. Louis, MO) or Cayman Chemicals (Ann Arbor, MI). VEA was synthesized in-house, as described.[13] Hemp oil extract (HOE) was obtained from Metagenics (www.metagenics.com).[14] LC/MS-grade water and methanol were from Honeywell (Muskegon, MI). LC/MS-grade acetonitrile, isopropanol, and acetone were from Sigma-Aldrich. Formic acid was from Thermo Fisher (Houston, TX).

Standard preparation

Stock solutions containing authentic THC, 11-OH-THC, 11-COOH-THC, CBD, anandamide, 2-AG, OEA, VEA, PEA, and [^{2}H]-containing internal standards (ISTD) were prepared in methanol (1.0 μg/mL). Serial dilutions in methanol (from 1.0 μg/mL to 0.02 ng/mL) were used to generate calibration curves for both plasma and brain after having determined experimentally that no matrix effects occurred.

Equipment

Chromatographic separations were carried out using a 1260 series LC system (Agilent Technologies, Santa Clara, CA) consisting of a binary pump, degasser, temperature-controlled autosampler, and column compartment, coupled to a 6460C triple quadrupole mass spectrometric detector with a Jet Stream electrospray ionization (ESI) interface.

Animals

Male and female C57BL/6 mice (postnatal day [PND], at arrival, 21) were purchased from Charles River (Wilmington, MA). They were group-housed (4 per cage) on a 12-h reverse light/dark cycle (lights on at 06:30 PM) with *ad libitum* food and water. All procedures were approved by the University of California Irvine Institutional Animal Care and Use Committee and were in accordance with the National Institute of Health guidelines for the Care and Use of Laboratory Animals.

Drug and treatments

THC and HOE were dissolved in a vehicle consisting of Tween80/saline (5:95, v/v).[15] Adolescent (PND 37) male and female mice received a single intraperitoneal injection of THC (5 mg/kg), HOE (100 mg/kg), HOE plus THC (20:1, v/v, 100 mg/kg HOE and 5 mg/kg THC), or vehicle. Tissue collections were performed as previously described.[9,13,16] Briefly, the animals were anesthetized with isoflurane 1 h after injections, blood was collected by cardiac puncture into ethylenediaminetetraacetic acid (EDTA)-rinsed syringes and transferred into 1 mL polypropylene plastic tubes containing spray-coated potassium-EDTA. Plasma was prepared by centrifugation at 1450×*g* at 4°C for 15 min and transferred into polypropylene tubes. The animals were decapitated, and their brains quickly removed. All tissue samples were immediately frozen on dry ice and stored at −80°C until analyses.

LC conditions

Initial method development was performed using an Eclipse XDB C18 (1.8 μm, 2.1×50 mm), monomeric

bonded phase (Agilent Technologies, Wilmington, DE). Further development was carried out using an Eclipse PAH C18, polymeric bonded phase (1.8 μm, 2.1 × 50 mm; Agilent Technologies, Wilmington, DE). The mobile phase consisted of water containing 0.1% formic acid as solvent A and methanol containing 0.1% formic acid as solvent B. The flow rate was kept at 0.3 mL/min. For Eclipse XDB C18, different gradient conditions were used, with gradient times of 5, 10, and 15 min with 60% B to 95% B. The gradient conditions for the Eclipse PAH column were as follows: starting 70% B to 80% B in 10.0 min, changed to 95% B at 10.01 min, and maintained till 2.5 min to remove any strongly retained materials from the column. Equilibration time was 2.5 min. Total analysis time, including re-equilibrium, was 15 min. Column temperature was maintained at experimentally determined optimal 40°C, and the autosampler at 9°C. Injection volume was 1.0 μL.

To prevent carryover, the needle was washed in the autosampler port for 10 sec before each injection using a wash solution consisting of 10% acetone in a solution consisting of water/methanol/isopropanol/acetonitrile (1:1:1:1, v/v).

MS conditions

The mass spectrometric detector (MSD) was operated in the positive ESI mode and analytes were quantified by dynamic multiple reaction monitoring (dMRM) using the transitions and time segments reported in Table 1. dMRM uses retention time segments, with analyte-specific MRMs, for data acquisition allowing the isolation of isobaric compounds with identical MRM transitions (e.g., OEA and VEA). Replicate analyses were performed to determine the average retention times of analytes for use under dMRM conditions. The scan time (ΔT) for each analyte was experimentally determined to ensure complete integration

Table 1. Mass Spectrometry Parameters of the Method

Analyte	Retention time (minutes)	Precursor ion (m/z)	Product ion (m/z)	Fragmentation voltage (V)	Collision energy (V)
[$^2H_3$]-11-OH-THC[a]	2.1	334.20	316.1	140	10
[$^2H_3$]-11-OH-THC[b]	2.1	334.20	105.1	140	50
11-OH-THC[a,c]	2.1	331.23	313.1	133	9
11-OH-THC[b]	2.1	331.23	105.0	133	45
[$^2H_3$]-11-COOH-THC	2.4	348.20	330.2	144	13
11-COOH-THC[a,c]	2.4	345.20	327.2	142	13
11-COOH-THC[b]	2.4	345.20	299.2	142	17
[$^2H_3$]-CBD[a]	3.4	318.20	196.2	150	22
[$^2H_3$]-CBD[b]	3.4	318.20	123.0	150	38
CBD[a]	3.4	315.20	193.1	138	21
CBD[b]	3.4	315.20	123.0	138	37
[$^2H_3$]-THC[a]	6.1	318.20	196.1	145	10
[$^2H_3$]-THC[b]	6.1	318.20	93.1	145	22
THC[a,c]	6.1	315.20	193.1	147	21
THC[b]	6.1	315.20	123.0	147	37
[$^2H_4$]-Anandamide[a,c]	7.0	352.32	66.2	140	50
[$^2H_4$]-Anandamide[b]	7.0	352.32	67.1	140	14
Anandamide[a]	7.0	348.29	62.2	128	13
Anandamide[b]	7.0	348.29	91.1	128	45
[$^2H_5$]-2-AG[a,c]	7.6	384.30	287.2	125	10
[$^2H_5$]-2-AG[b]	7.6	384.30	67.1	125	50
2-AG[a]	7.6	379.29	287.2	123	10
2-AG[b]	7.6	379.29	269.2	123	13
VEA[a]	10.0	326.30	62.1	120	14
VEA[b]	10.0	326.30	55.1	133	42
[$^2H_4$]-OEA[a,c]	10.3	330.34	66.1	140	14
[$^2H_4$]-OEA[b]	10.3	330.34	312.8	140	22
OEA[a]	10.3	326.31	62.1	133	13
OEA[b]	10.3	326.31	55.1	133	45
[$^2H_4$]-PEA[a,c]	12.6	304.32	66.2	125	14
[$^2H_4$]-PEA[b]	12.6	304.32	287.2	125	18
PEA[a]	12.6	300.29	62.2	128	13
PEA[b]	12.6	300.29	57.1	128	33

[a]Quantifier.
[b]Qualifier.
[c]Used in matrix effect studies.
11-COOH-THC, 11-nor-9-carboxy-Δ^9-THC; 11-OH-THC, 11-hydroxy-Δ^9-THC; 2-AG, 2-arachidonoyl-*sn*-glycerol; CBD, cannabidiol; OEA, oleoylethanolamide; PEA, palmitoylethanolamide; THC, Δ^9-tetrahydrocannabinol; VEA, vaccenoylethanolamide.

of the peaks, approximately twice their peak widths obtained under MRM.

Acquisition parameters were optimized for each analyte using the Agilent MassHunter Optimizer software (Table 1). Source parameters were also optimized using the Agilent MassHunter. Nebulizer and sheath gas temperatures were each set at 300°C with flow rates of 9.0 and 12.0 L/min, respectively. Nebulizer pressure was 50 psi. Capillary and nozzle voltages were set at 3000 and 1900 V, respectively. The MassHunter software was used for instrument control, data acquisition, and analysis.

Sample preparation

Samples were prepared as previously described.[16–20] Briefly, plasma (0.1 mL) was transferred into 8 mL glass vials (catalog no.: B7999-3; Thermo Fisher) and proteins were precipitated by adding 0.5 mL of ice-cold acetonitrile containing 1% formic acid and ISTD. Frozen whole brains were pulverized on dry ice using a mortar and pestle. Aliquots of tissue (20–25 mg) were homogenized using a Precellys CK-14 soft tissue homogenizing kit (Bertin Corp., Rockville, MD) in a Precellys Evolution apparatus at 4°C on preset setting #4 (6500 RPM × 20 sec × 2) in 0.5 mL of ice-cold acetonitrile containing 1% formic acid and ISTD. Plasma and brain samples were stirred vigorously for 30 sec and centrifuged at 2800 × *g* at 4°C for 15 min.

After centrifugation, the supernatants were loaded onto Captiva-Enhanced Matrix Removal (EMR)-Lipid cartridges (Agilent Technologies, Wilmington, DE) and eluted under positive pressure (3–5 mmHg, 1 drop/5 sec; positive pressure manifold 48 processor; Agilent Technologies, Wilmington, DE). For brain fractionation, EMR cartridges were prewashed with water/acetonitrile (1:4, v/v). No pretreatment was necessary for plasma fractionation. Tissue pellets were rinsed with water/acetonitrile (1:4, v/v; 0.2 mL), stirred for 30 sec, and centrifuged at 2800 × *g* at 4°C for 15 min. The supernatants were collected, transferred onto EMR cartridges, eluted, and pooled with the first eluate. The cartridges were washed again with water/acetonitrile (1:4, v/v; 0.2 mL), and the pressure was increased gradually to 10 mmHg (1 drop/sec) to ensure maximal analyte recovery.

Eluates were dried under N_2 and reconstituted in 0.1 mL of methanol containing 0.1% formic acid. Samples were transferred to deactivated glass inserts (0.2 mL) placed inside amber glass vials (2 mL; Agilent Technologies, Wilmington, DE).

Limits of detection and quantification

The lower limit of detection (LLOD) and lower limit of quantification (LLOQ) were determined using a signal-to-noise ratio of ≥ 3.0 and ≥ 10.0, respectively. The upper limit of quantification was 500 ng/mL for all analytes.

Precision, accuracy, and recovery

Three replicates of 3 quality control (QC) samples (5, 50, and 200 ng/mL) were prepared as prespiked (Set A) and postspiked EMR (Set B) plasma and brain from naive adolescent female mice and were used to determine accuracy and precision. Three replicates of a nonspiked QC sample were used to determine baseline analyte concentrations. Each QC sample was run in triplicate on 3 separate days along with calibration curves, to determine interday accuracy and precision. Precision was evaluated by calculating percent relative standard deviation (%RSD) of sample replicates within each day. Accuracy was determined as relative percent error from a nominal concentration and calculated as follows: [(measured concentration)/(nominal concentration)] × 100. Recovery was calculated as (Set B/Set A) × 100. Brain samples were analyzed and then further diluted 10 × and 25 × to allow accurate 2-AG quantification.

Following the Food and Drug Administration (FDA) Bioanalytical Method Validation Guidelines, acceptable mean values for precision and accuracy were ± 15% of the actual value and ± 20% for limit of quantification.[21]

Matrix effect

Potential matrix effects were evaluated using a postcolumn infusion method.[22] Because target analytes are present endogenously in the matrix and brain, deuterium-containing [$^2H_5$]-2-AG, [$^2H_3$]-AEA, [$^2H_3$]-OEA, and [$^2H_3$]-PEA were used for the study. Matrix effects for THC, THC-OH, and THC-COOH were evaluated using their quantifier MRMs. VEA and CBD were not studied separately because they have the same MRM transitions as OEA and THC, respectively. One milliliter each of 10 μM solutions in methanol containing 0.1% formic acid was loaded onto 1 mL syringes. They were infused into the MSD using a syringe pump attached through a T-connector that combined the postcolumn flow with the LC column flow. The infusion rate was 0.3 mL/h, and baseline responses were monitored using the transitions described in Table 1.

After a steady-state MSD response was reached, 2.0 μL of pre-EMR or post-EMR plasma or brain extracts was injected and data were acquired under optimized chromatographic conditions. Superimposing the resulting pre- and post-EMR matrix profiles with the chromatograms of target analytes identified regions of potential matrix-induced ion suppression or enhancement.

Statistical analyses

Sex- and treatment-dependent differences in method application experiments were analyzed using two-way analysis of variance with Bonferroni *post hoc* test. Differences between groups were considered statistically significant at values of $p < 0.05$.

Results

Phase and temperature selectivity

We first attempted to separate mixtures of phytocannabinoids (CBD, THC, and its major oxidative metabolites), endocannabinoids (anandamide, 2-AG, and its positional isomer 1-AG), and paracannabinoids (OEA and PEA) using a monomeric bonded phase (Eclipse XDB C18), which allows baseline separation of analytes within each of these classes.[14,18,22,23]

Despite multiple mobile phase and gradient modifications, 2-AG, 1-AG, and PEA were not satisfactorily resolved (Fig. 2, data not shown). We turned therefore to a polymeric bonded C18 column (Eclipse PAH C18), which is used to separate polycyclic aromatic hydrocarbons and other rigid organic molecules by leveraging temperature-dependent shape selectivity.[24] We evaluated 4 progressively lower temperatures (50°C, 45°C, 40°C, and 35°C). Figure 3 shows separation of target analytes at 50°C, 45°C, and 40°C (35°C is omitted for clarity). At 50°C, OEA and PEA coeluted (Fig. 3A), but resolution improved as the temperature was progressively decreased to 45°C and 40°C (Fig. 3B, C).

Greater resolution was obtained at 35°C, but with an unacceptable increase in separation time (not shown). The best compromise between analyte resolution and run time was achieved at 40°C (Fig. 3C). At this temperature, all target analytes eluted in < 14 min and exhibited both greater-than-baseline resolution (> 1.5) and symmetric peak shapes (only PEA produced some tailing). OEA (Δ^9-octadecaenoylethanolamide) and

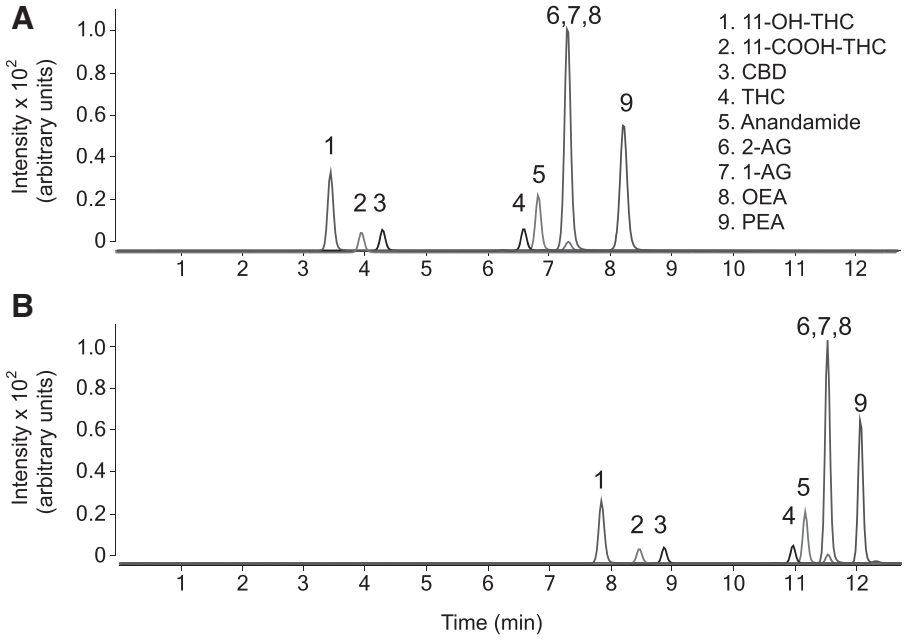

FIG. 2. Representative extracted ion chromatograms showing LC separation of 11-OH-THC (1), 11-COOH-THC (2), CBD (3), THC (4), anandamide (5), 2-AG (6), 1-AG (7), PEA (8), and OEA (9) using Eclipse XDB C18 column with a 5-min gradient **(A)** or 15-min gradient **(B)**. Despite multiple gradient modifications, 2-AG, 1-AG, and PEA coeluted from the LC column.

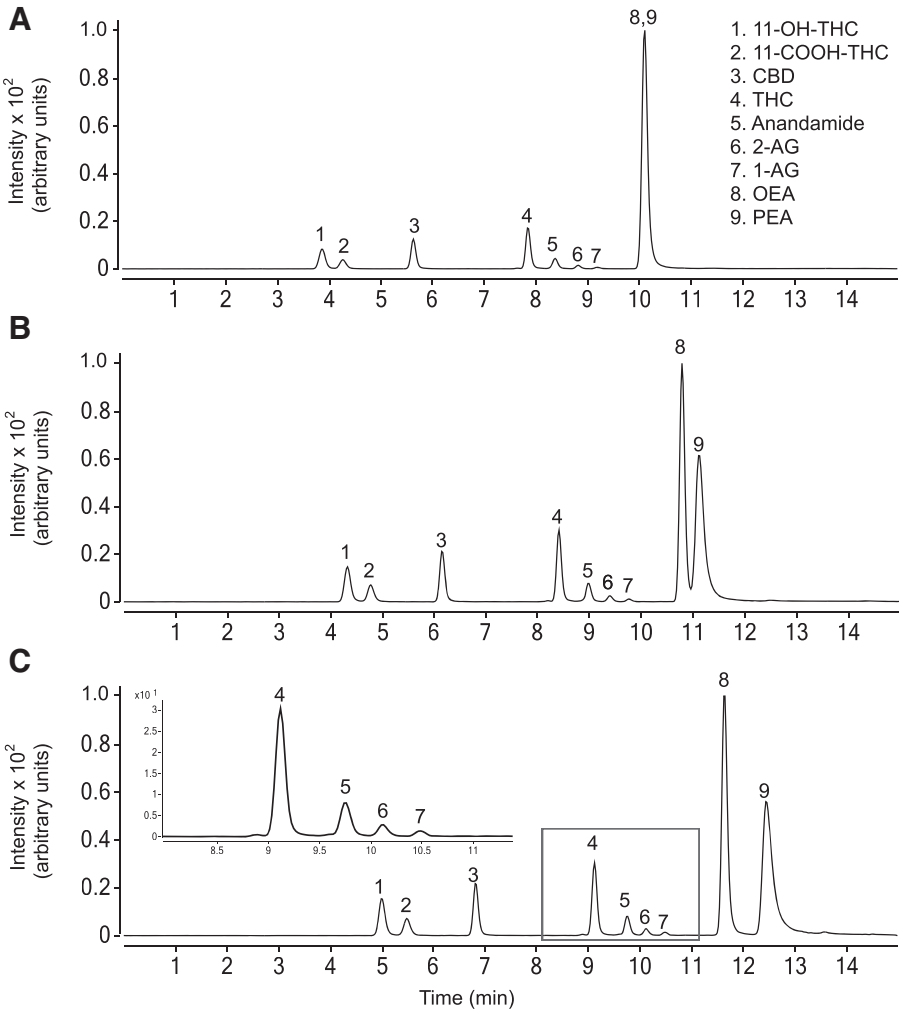

FIG. 3. Representative extracted chromatograms showing LC separation of 11-OH-THC (1), 11-COOH-THC (2), CBD (3), THC (4), anandamide (5), 2-AG (6), 1-AG (7), OEA (8), and PEA (9) at column temperatures of 50°C **(A)**, 45°C **(B)**, and 40°C **(C)**. Inset of (C) shows 10× magnification of tracing contained in the box.

VEA (Δ^{11}-octadecaenoylethanolamide), which are isobaric regioisomers, required additional optimization. After establishing the best temperature for the separation of other analytes, we introduced incremental modifications to the gradient and eventually achieved a 0.6–0.7 resolution with a gradient that started with 70% solvent B (Fig. 4). Under these conditions, resolution between THC-OH and THC-COOH decreased to 1.2 (from the original 1.5), while resolution of other analytes was not affected (Table 2). Since OEA and VEA have identical MRM transitions (Table 1), we used dMRM to quantify them separately.

Quantification

Curve linearity for all analytes was determined in the absence of matrix using a $1/x^2$ weighting factor. R^2 values, LLOD, and LLOQ for all analytes are shown in Table 3. Accuracy values for the concentration ranges of the calibration curves were 80–120%, which are within the FDA bioanalysis guidelines.[21]

Precision, accuracy, and recovery

Average interday precision and accuracy were determined for all analytes in both plasma and brain matrix, before and after EMR fractionation. Three separate QC

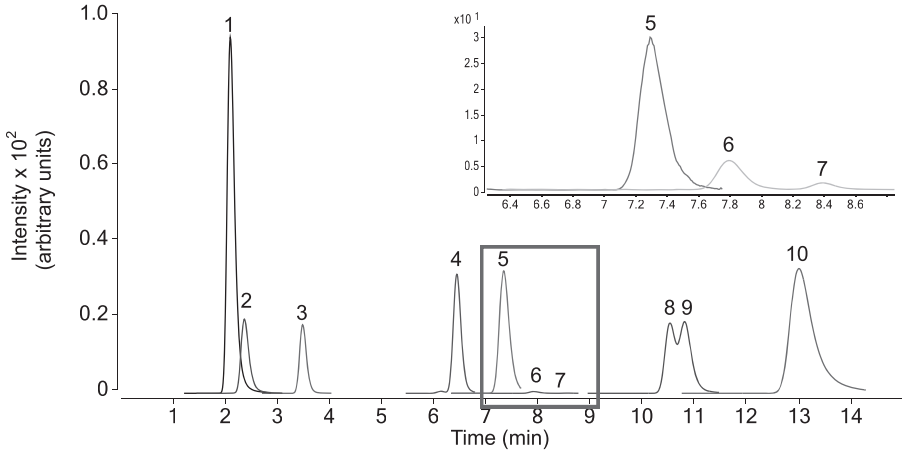

FIG. 4. Representative extracted ion chromatogram showing LC separation of 11-OH-THC (1), 11-COOH-THC (2), CBD (3), THC (4), anandamide (5), 2-AG (6), 1-AG (7), VEA (8), OEA (9), and PEA (10) at 40°C column temperature under dMRM conditions. Inset shows 10× magnification of tracing contained in the box. dMRM, dynamic multiple reaction monitoring.

samples at 3 standard analyte concentrations (5, 50, and 200 ng/mL) were prepared and run in triplicate on 3 consecutive days. Precision was determined by calculating %RSD. Accuracy was determined as relative percent error on nominal quantity. Accuracy and precision values for pre-EMR and post-EMR plasma containing QC samples are reported in Table 4 and Supplementary Table S1, respectively. Corresponding values for the brain are shown in Supplementary Tables S2 and S3. In all cases, accuracy and precision were within the FDA recommendations (±15% of nominal concentration).[21] Recovery, which was determined as (Response precolumn/Response postcolumn)×100, ranged from 86.3% to 104.0% for plasma and from 86.2% to 104.2% for brain (Table 5).

Table 2. Liquid Chromatography Parameters of the Method

Peak ID	*k*	Peak width	Symmetry	Peak resolution		Log *p*
1. 11-OH-THC	4.38	1.3	0.71	—	—	6.58
2. 11-COOH-THC	5.01	1.1	0.54	COOH/OH	1.2	6.21
3. CBD	7.49	1.2	0.71	CBD/COOH	4.1	7.03
4. THC	14.09	1.2	0.70	THC/CBD	11.7	7.68
5. Anandamide	16.09	0.9	0.62	AEA/THC	2.9	5.67
6. 2-AG	17.36	1.1	0.68	2-AG/AEA	1.6	6.25
7. 1-AG	18.82	1.2	1.10	1-AG/2-AG	1.9	6.02
8. VEA	23.23	1.2	1.33	VEA/1-AG	4.9	6.36
9. OEA	23.85	1.2	0.47	OEA/VEA	0.6	6.36
10. PEA	28.63	2.1	0.42	PEA/OEA	3.0	5.82

Matrix effect

Figure 5 illustrates the results obtained when post-EMR extracts of mouse plasma and brain tissue were chromatographed according to the present method while monitoring the MRM transition for [$^2H_4$]-anandamide ($m/z = 352.32 > 66.2$; Fig. 5A) or [$^2H_5$]-2-AG ($m/z = 384.3 > 287.2$; Fig. 5B). Deuterium-containing standards were used in this experiment because plasma and brain tissues contain substantial amounts of native anandamide and 2-AG. We did not observe any regions of ion suppression or enhancement for any of the analytes tested (Supplementary Fig. S1), confirming our previous data indicating that EMR fractionation is effective in removing the matrix components that would otherwise interfere with the analysis.[18]

Method application

We tested the new method by analyzing plasma and brain extracts from adolescent male and female mice that had received a single injection of THC (5 mg/kg, i.p.), HOE (100 mg/kg), HOE:THC (100/5 mg/kg), or their vehicle and were euthanized 1 h later. Figure 6 reports representative extracted-ion chromatograms for the brain from female animals treated with vehicle (Fig. 6A) or the HOE:THC combination (Fig. 6B). The tracings show the elution of THC, its oxidative products (11-OH-THC and 11-COOH-THC), endocannabinoids (anandamide, 2-AG, and its isomer 1-AG), paracannabinoids (PEA, OEA), and the naturally occurring isomer of

Table 3. Calibration Curve Parameters, Weighted at $1/x^2$

Analyte	R^2	LLOD (ng/mL)	fmol/injection[b]	LLOQ (ng/mL)	fmol/injection[b]
11-OH-THC	0.996	0.05	0.15	0.1	0.3
11-COOH-THC	0.992	0.2	0.58	0.5	1.45
CBD	0.999	0.1	0.32	0.2	0.64
THC	0.989	0.1	0.32	0.2	0.64
Anandamide	0.989	0.02	0.06	0.05	0.15
2-AG[a]	0.988	0.5	1.32	1.0	2.64
VEA	0.987	0.02	0.06	0.05	0.12
OEA	0.998	0.05	0.15	0.1	0.30
PEA	0.989	1.0	3.3	2.0	6.6

LLOD and LLOQ were determined using a signal-to-noise ratio of ≥ 3.0 and ≥ 10.0, respectively.
[a]2-AG and 1-AG combined.
[b]On column concentration based on 1.0 μL injection.
LLOD, lower limit of detection; LLOQ, lower limit of quantification.

OEA, VEA. 1-AG is produced from 2-AG through acyl migration, which primarily occurs during sample preparation and storage.[25,26] Analyte concentrations for plasma and brain, which are listed in Tables 6 and 7, respectively, are within the range expected from literature data.[14,17,25]

Female mice treated with THC exhibited higher concentrations of 11-OH-THC in both plasma and brain compared with males (58.41 ± 10.2 vs. 29.16 ± 5.56 ng/mL, $p < 0.05$, plasma; 188.37 ± 13.34 vs. 106.83 ± 23.75 ng/g, $p < 0.05$, brain). THC administration increased the circulating concentrations of anandamide, VEA, and OEA in both male and female animals (Table 6), which is consistent with the literature.[6–9]

Discussion

This study describes a sensitive and easily implementable UHPLC-MS/MS method for the simultaneous

Table 4. Interday Accuracy and Precision of Analyte Quantification in Pre-Enhanced Matrix Removal Spiked Plasma

Measured amount (ng/mL)

Nominal quantity (ng/mL)	Analyte	Day 1			Day 2			Day 3		
		Mean	%RSD	Accuracy (%)	Mean	%RSD	Accuracy (%)	Mean	%RSD	Accuracy (%)
5	OH-THC	4.24	1.55	84.88	4.69	2.61	93.86	4.39	1.78	87.74
	COOH-THC	4.48	2.10	89.62	4.27	1.92	85.39	4.42	2.40	88.44
	CBD	4.60	0.11	92.06	4.46	1.79	89.19	4.45	2.34	89.04
	THC	4.34	1.16	86.84	4.38	2.13	89.52	4.33	0.09	86.55
	Anandamide	5.37	2.83	97.68	5.39	1.32	97.79	5.46	2.41	99.28
	2-AG	13.61	4.39	108.89	14.56	8.90	96.10	16.03	6.01	105.15
	VEA	6.23	1.08	102.60	6.47	2.46	106.91	6.18	1.90	101.69
	OEA	6.34	0.79	96.09	6.29	4.04	95.76	6.33	0.07	96.07
	PEA	9.90	13.14	107.25	9.89	8.94	108.89	10.06	10.85	108.14
50	OH-THC	50.92	3.04	101.84	56.89	1.64	113.79	51.18	3.06	102.35
	COOH-THC	50.84	4.25	101.68	49.98	2.12	99.96	50.96	2.01	101.92
	CBD	50.99	4.36	101.98	50.75	1.09	101.49	51.90	1.36	103.81
	THC	50.64	3.35	101.27	53.83	3.91	107.66	51.28	1.92	102.56
	Anandamide	50.65	2.35	100.30	50.55	2.34	100.07	50.14	1.98	99.27
	2-AG	58.13	6.47	101.11	57.81	8.11	96.11	55.00	4.91	91.29
	VEA	52.92	1.05	86.19	55.71	7.41	109.12	51.67	2.11	101.18
	OEA	50.64	3.35	98.13	53.83	3.91	104.39	51.28	1.95	99.41
	PEA	52.21	2.63	96.28	48.70	2.77	90.05	50.93	3.73	93.78
200	OH-THC	205.27	0.97	102.63	228.44	1.43	114.22	210.33	1.43	105.17
	COOH-THC	208.68	1.07	104.35	204.64	1.14	102.33	216.06	0.86	107.86
	CBD	211.56	0.77	105.78	205.55	1.20	102.77	211.28	0.37	105.64
	THC	213.17	0.56	106.59	220.48	1.98	110.24	207.81	3.94	103.90
	Anandamide	228.14	1.45	113.78	227.87	0.98	113.78	225.68	0.86	112.56
	2-AG	247.13	0.73	119.10	241.70	2.27	115.01	235.65	1.19	112.08
	VEA	203.30	0.86	101.11	198.99	0.78	98.97	194.01	0.17	96.49
	OEA	227.13	0.79	112.66	221.70	2.48	109.99	215.65	1.29	106.98
	PEA	231.97	1.98	113.59	223.25	8.09	109.39	231.56	4.36	113.34

Analyses were run on 3 consecutive days. The standard error of the mean was in all cases $\leq 20\%$ and was omitted for clarity.
%RSD, percent relative standard deviation; EMR, Enhanced Matrix Removal.

Table 5. Analyte Recovery Following Enhanced Matrix Removal Fractionation from Plasma or Brain Tissue

[ng/mL]	Analyte	Plasma Recovery (%)	Brain Recovery (%)
5	OH-THC	95.2	91.9
	COOH-THC	96.9	98.4
	CBD	88.5	92.2
	THC	87.7	90.4
	Anandamide	93.7	88.5
	2-AG	94.3	94.3
	VEA	98.9	90.5
	OEA	101.6	88.2
	PEA	101.6	86.2
50	OH-THC	88.4	102.0
	COOH-THC	90.8	99.0
	CBD	86.0	98.9
	THC	86.7	102.6
	Anandamide	87.3	104.2
	2-AG	100.8	100.8
	VEA	86.2	100.9
	OEA	94.6	99.1
	PEA	85.6	95.9
200	OH-THC	101.5	92.1
	COOH-THC	93.6	93.5
	CBD	102.2	91.8
	THC	101.0	94.9
	Anandamide	91.3	93.6
	2-AG	93.9	94.0
	VEA	86.3	99.8
	OEA	104.0	90.1
	PEA	104.0	100.5

Recovery (%) was calculated as (Response pre-EMR/Response post-EMR) × 100, where response pre-EMR is the average area for the analytes, which have gone through the fractionation process. Response post-EMR is the average area for the same quantity of analyte spiked into the extracted matrix after the fractionation procedure ($n = 3$/condition, run in duplicate).

identification and quantification of two primary phytocannabinoids (THC and CBD), a selection of prominent THC metabolites (11-OH-THC, 11-COOH -THC), and several endogenous signaling molecules belonging to the endocannabinoid and paracannabinoid families of lipid mediators.[1] Many methods are available for the separate analysis of each of these classes[18,25–29] or for the untargeted analysis of these compounds in complex lipid mixtures.[30] However, chemical differences among such classes pose a challenge to the analyst who intends to compare—easily, quantitatively, accurately, and rapidly—levels of these constituents in biological samples.

The present protocol leverages the temperature-dependent shape selectivity properties offered by polymeric bonded C18 phases to achieve temperature-dependent separation of 9 quantitatively significant members of these classes in a single chromatographic run.

Understanding the impact of cannabis use on the endocannabinoid and paracannabinoid systems is important because the two most abundant phytocannabinoids, THC and CBD, are known to engage these signaling complexes either directly (THC, by activation of cannabinoid receptors) or indirectly (CBD, by modulating cannabinoid receptor activity or anandamide degradation).[31] For example, pre-clinical and clinical studies have shown that administration of either THC or CBD affects the concentrations of anandamide, OEA, and PEA in circulation.[6–9] It is possible that these alterations contribute to the short- and long-term effects of cannabis, but this hypothesis has not been fully tested yet. As ongoing societal changes expose new sectors of the population to cannabis—including groups at unknown risk such as adolescents, pregnant women, and the elderly[11,12]—it is important to fill this knowledge gap.

A crucial step toward achieving this goal is to develop practical methods to measure phytocannabinoid, endocannabinoid, and paracannabinoid compounds in relevant biological matrices. One such method was recently developed,[29] which does not effectively separate all analytes and does not include analytes of interest such as the first oxidative and psychoactive metabolite of THC, 11-OH-THC,[15–20] and VEA, the isobaric analogue of OEA. Such high-resolution separations are necessary to accurately quantitate these analytes, with very similar mass and fragmentation patterns, in complex biological matrices. Moreover, a lipidomic method that monitors >100 phytocannabinoids and endogenous lipid-derived molecules has been reported.[31] Such method is useful for untargeted applications but would be impractical for more focused ones because (a) it requires high-resolution MS/MS; and (b) it does not leverage isotope-dilution quantification of targeted analytes, as required for optimal quantification.

Although focused on phytocannabinoids and endocannabinoids, the present method also allows the quantification of OEA and PEA, two endogenous peroxisome proliferator-activated receptor-α (PPAR-α) agonists that serve important functions in the control of pain, inflammation, and energy balance.[31–36] These bioactive lipid amides can act either synergistically or antagonistically with endocannabinoid signals. For example, they attenuate nociception in animal models[37–39] and enhance the antinociceptive effects of anandamide,[40,41] but counter its appetite-stimulating actions.[42] Both responses are mediated by PPAR-α activation.[38,42] The present method also includes VEA and 1-AG. VEA is a naturally occurring regioisomer of OEA that can confound the latter's quantification,[43–45]

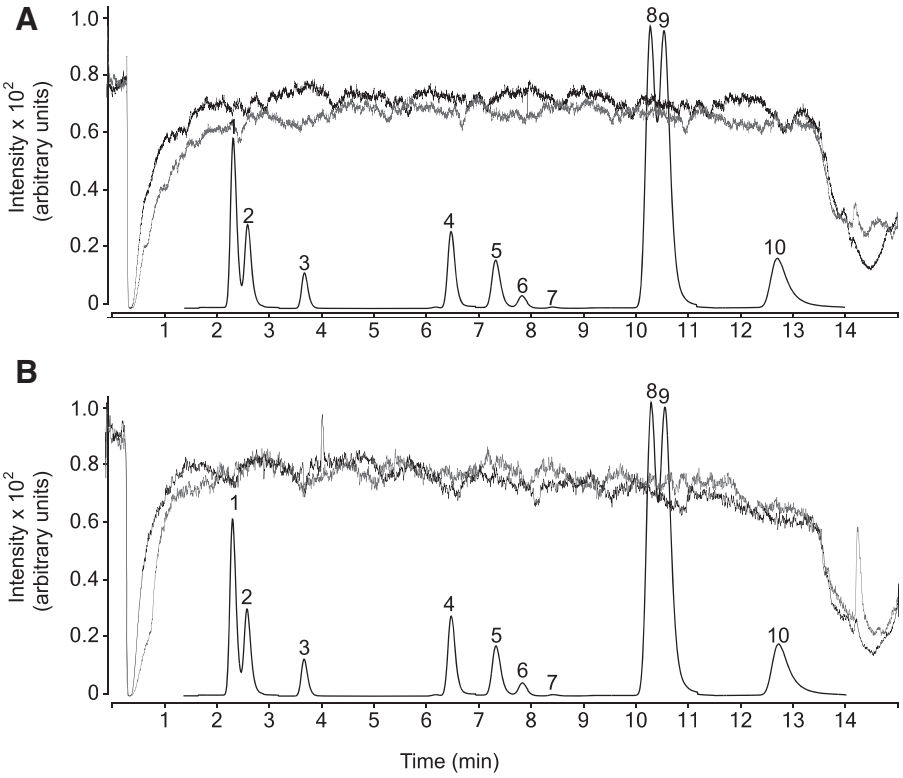

FIG. 5. Post-EMR matrix effect for [$^2H_4$]-anandamide **(A**; peak 5**)** or [$^2H_5$]-2-AG **(B**; peak 6**)** in plasma (grey) and brain (black). EMR, Enhanced Matrix Removal.

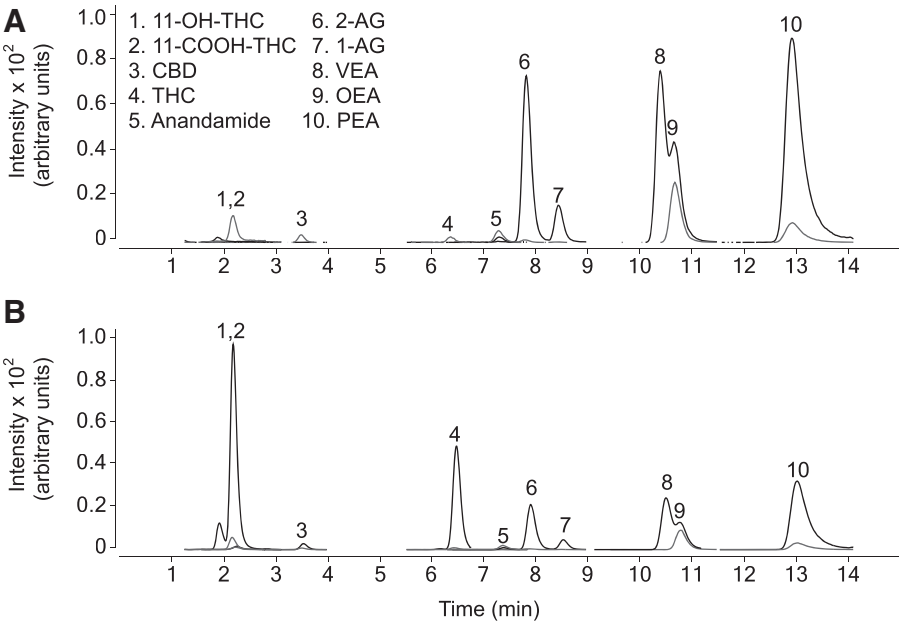

FIG. 6. Representative extracted ion chromatograms showing LC separation of 11-OH-THC (1), 11-COOH-THC (2), CBD (3), THC (4), anandamide (5), 2-AG (6), 1-AG (7), VEA (8), OEA (9), and PEA (10), in brain tissue 1 h after administration of vehicle **(A)** or HOE:THC **(B)** to adolescent female mice (PND 37). Black tracing shows analytes of interest, grey, lower peaks tracing shows deuterium-labeled internal standards. HOE, hemp oil extract; PND, postnatal day.

Table 6. Analyte Concentrations in Plasma of Adolescent (Postnatal Day 37; $n = 5$) Male and Female Mice 1 H After Intraperitoneal Administration of Vehicle (5:95 Tween80/Saline, 5:95, v/v), THC (5 mg/kg), HOE (100 mg/kg), or HOE:THC (100/5 mg/kg)

		VEH		THC (5 mg/kg)		HOE (100 mg/kg)		HOE:THC 20:1	
Peak	Analyte	Males (ng/mL)	Females (ng/mL)	Males (ng/mL)	Females (ng/mL)	Males (ng/mL)	Females (ng/mL)	Males (ng/mL)	Females ng/mL)
1	11-OH-THC	ND	ND	29.16	58.41$^{\#}$	ND	ND	31.51	30.20
2	11-COOH-THC	ND	ND	73.67	74.68	ND	ND	95.16	94.60
3	CBD	ND	ND	ND	ND	53.52	136.49	65.00	61.31
4	THC	ND	ND	112.51	123.90	ND	ND	164.37	160.81
5	Anandamide	0.51	0.75	0.72	1.32$^{**,\#\#}$	0.57	0.82	0.64	0.65
6+7	2-AG	16.95	14.25	18.90	13.25	19.51	14.14	20.13	15.08
8	VEA	0.34	0.32	0.46*	0.45*	0.35	0.36	0.40	0.30
9	OEA	0.31	0.43	0.42	0.51	0.37	0.51	0.44	0.43
10	PEA	11.65	14.91	14.98	14.40	13.85	14.04	18.00*	12.78

*Denotes significance compared with vehicle. $^{\#}$Denotes significance by sex. * or $^{\#}p < 0.05$, ** or $^{\#\#}p < 0.01$, two-way ANOVA with Bonferroni *post hoc* analysis. The standard error of the mean was in all cases ≤30% and was omitted for clarity.

ANOVA, analysis of variance; HOE, hemp oil extract; ND, nondetectable; VEH, vehicle.

while 1-AG is predominantly generated by 2-AG isomerization ("acyl shift") occurring during sample preparation.[25,26]

The fractionation of these structurally related analytes was made possible by temperature-dependent shape selectivity. This term denotes a quality exhibited by certain LC stationary phases, which allows them to resolve solutes based on their molecular structures, rather than other physical or chemical properties.[23] Various models have been proposed to explain shape selectivity.[24, 46–53] According to one model,[47] solute retention is determined by the formation of analyte-sized cavities in the stationary phase, with bulkier analytes requiring more energy for retention. We cannot fully rationalize the order of analyte elution yielded by our method (Fig. 1), but some considerations are plausible. The presence of polar moieties in products of oxidative THC metabolism, 11-OH-THC and 11-COOH-THC, may explain their shorter retention times.

A similar effect may be produced by the rigid terpenophenolic structures of phytocannabinoids, especially THC (Fig. 1), which might result in their incomplete insertion into the stationary C18 phase and thus in faster elution compared with endocannabinoid and paracannabinoid fatty acyl derivatives.[46] The pairs anandamide/2-AG and 2-AG/1-AG tend to resolve better at higher temperature, whereas the pair OEA/PEA shows a linear, temperature-dependent decrease in resolution. OEA, although less polar than PEA, elutes first possibly because of the steric effect produced by the presence of a double bond in *cis* configuration (Fig. 1).

Table 7. Analyte Concentrations in Plasma of Adolescent (Postnatal Day 37; $n = 5$) Male and Female Mice 1 H After Intraperitoneal Administration of Vehicle (5:95 Tween80/Saline, 5:95, v/v), THC (5 mg/kg), HOE (100 mg/kg), or HOE:THC (100/5 mg/kg)

		VEH		THC (5 mg/kg)		HOE (100 mg/kg)		HOE:THC 20:1	
Peak	Analyte	Males (ng/g)	Females (ng/g)	Males (ng/g)	Females (ng/g)	Males (ng/g)	Females (ng/g)	Males (ng/g)	Females (ng/g)
1	11-OH-THC	ND	ND	106.82	188.37$^{\#}$	ND	ND	123.56	188.16
2	11-COOH-THC	ND	ND	17.93	18.93	ND	ND	17.12	17.30
3	CBD	ND	ND	ND	ND	68.53	62.23	59.61	51.18
4	THC	ND	ND	261.03	198.48	ND	ND	307.35	307.57
5	Anandamide	2.79	3.42	2.94	3.60	2.72	3.68	3.10	3.31
6+7	2-AG	9461.22	12,322.85	8743.13	11,212.47	10,994.10	10,169.30	11,795.73	10,653.38
8	VEA	4.10	5.92$^{\#}$	5.34	5.53	4.64	5.47	5.54	5.41
9	OEA	1.81	3.17$^{\#\#}$	2.19	2.29	2.17	2.18*	3.28*	1.96$^{*,\#\#}$
10	PEA	80.41	134.14$^{\#}$	88.91	87.85	81.85	99.99	139.16*	85.85$^{\#}$

*Denotes significance compared with vehicle. $^{\#}$Denotes significance by sex. * or $^{\#}p < 0.05$, or $^{\#\#}p < 0.01$, two-way ANOVA with Bonferroni *post hoc* analysis. The standard error of the mean was in all cases ≤30% and was omitted for clarity.

Of note, the present method partially resolves OEA from its regioisomer VEA, which is normally present in rodent and human samples[53] but does not appear to participate in paracannabinoid signaling.[43] The faster elution of VEA might be a consequence of an incomplete insertion of its tail end (the alkyl chain after the Δ^{11} double bond) into the C18 bonded phase. Thus, the retention of endocannabinoid and paracannabinoid analytes might be dominated by the steric selectivity of their nonpolar tails, which might account for the finding that they do not elute according to the calculated log *p* values (Table 3).

The current study has two main limitations. First, our lowest QC tested was 5.0 ng/mL. This value was chosen because it is a concentration that produces a robust signal for all analytes, specifically PEA and 2-AG, which have an LLOQ of 2.0 and 1.0 ng/mL, respectively. Second, we did not test for possible interferences from other minor cannabinoids such as cannabichromene or cannabigerol. Neither cannabinoids were detectable in our HOE,[14] but further method development to include a wider range of cannabinoids is currently underway.

In conclusion, we leveraged the temperature-dependent shape selectivity of the polymerically bonded C18 phase to develop a selective and easily implemented UHPLC-MS/MS method for the separation of a diverse mixture of endogenous and exogenous cannabinoid substances. The results underscore several issues that must be taken into consideration in the analysis of such compounds—including temperature dependence of LC selectivity and biological matrix effects. The development of robust analytical methods, such as the one presented in this study, is an essential step toward understanding the impact of cannabis use on the human body.

Acknowledgment

We thank Dakota Kenneth Grimes for assistance with tissue collection.

Authors' Contributions

F.A.: Conceptualization, formal analysis, methodology, validation, writing—original draft, and revision. A.T.: Formal analysis, validation, writing—original draft, and revision. S.V.M.: Resources and supervision. F.F.: Formal analysis and methodology. M.A.H.: Supervision and writing—original draft. D.P.: Conceptualization, methodology, supervision, writing—original draft, and revision.

Author Disclosure Statement

The authors declare that they have no known competing financial interests or personal relationships that could have appeared to influence the work reported in this article.

Funding Information

The study was funded by the National Institute on Drug Abuse (Center of Excellence Grant DA044118).

Supplementary Material

Supplementary Figure S1
Supplementary Table S1
Supplementary Table S2
Supplementary Table S3

References

1. Piomelli D, Mabou Tagne A. Endocannabinoid-based therapies. Annu Rev Pharmacol Toxicol 2022;62:483–507; doi: 10.1146/annurev-pharmtox-052220-021800
2. LoVerme J, Gaetani S, Fu J, et al. Regulation of food intake by oleoylethanolamide. Cell Mol Life Sci 2005;62:708–716; doi: 10.1007/s00018-004-4494-0
3. Tovar R, Gavito AL, Vargas A, et al. Palmitoleoylethanolamide is an efficient anti-obesity endogenous compound: Comparison with oleylethanolamide in diet-induced obesity. Nutrients 2021;13:2589; doi: 10.3390/nu13082589
4. LoVerme J, Fu J, Astarita G, et al. The nuclear receptor peroxisome proliferator-activated receptor-alpha mediates the anti-inflammatory actions of palmitoylethanolamide. Mol Pharmacol 2005;67:15–19; doi: 10.1124/mol.104.006353
5. Im DS. GPR119 and GPR55 as receptors for fatty acid ethanolamides, oleoylethanolamide and palmitoylethanolamide. Int J Mol Sci 2021;22:1034; doi: 10.3390/ijms22031034
6. Walter C, Ferreirós N, Bishay P, et al. Exogenous delta9-tetrahydrocannabinol influences circulating endogenous cannabinoids in humans. J Clin Psychopharmacol 2013;33:699–705; doi: 10.1097/JCP.0b013e3182984015
7. Maia J, Midão L, Cunha SC, et al. Effects of cannabis tetrahydrocannabinol on endocannabinoid homeostasis in human placenta. Arch Toxicol 2019;93:649–658; doi: 10.1007/s00204-019-02389-7
8. Leweke FM, Piomelli D, Pahlisch F, et al. Cannabidiol enhances anandamide signaling and alleviates psychotic symptoms of schizophrenia. Transl Psychiatry 2012;20:e94; doi: 10.1038/tp.2012.15
9. Ellgren M, Artmann A, Tkalych O, et al. Dynamic changes of the endogenous cannabinoid and opioid mesocorticolimbic systems during adolescence: THC effects. Eur Neuropsychopharmacol 2008;18:826–834; doi: 10.1016/j.euroneuro.2008.06.009
10. Miech RA, Patrick ME, O'Malley PM, et al. Trends in reported marijuana vaping among US adolescents, 2017–2019. JAMA 2020;23:475–476; doi: 10.1001/jama.2019.20185
11. Pacek LR, Mauro PM, Martins SS. Perceived risk of regular cannabis use in the United States from 2002 to 2012: Differences by sex, age, and race/ethnicity. Drug Alcohol Depend 2015;149:232–244; doi: 10.1016/j.drugalcdep.2015.02.009
12. Mauro PM, Carliner H, Brown QL, et al. Age differences in daily and nondaily cannabis use in the United States, 2002–2014. J Stud Alcohol Drugs 2018;79:423–431; doi: 10.15288/jsad.2018.79.423
13. Ghidini A, Scalvini L, Palese F, et al. Different roles for the acyl chain and the amine leaving group in the substrate selectivity of N-Acylethanolamine acid amidase. J Enzyme Inhib Med Chem 2021;36:1411–1423; doi: 10.1080/14756366.2021.1912035
14. Mabou Tagne A, Fotio Y, Lin L, et al. Palmitoylethanolamide and hemp oil extract exert synergistic anti-nociceptive effects in mouse models of

acute and chronic pain. Pharmacol Res 2021;167:105545; doi: 10.1016/j.phrs.2021.105545
15. Burston JJ, Wiley JL, Craig AA, et al. Regional enhancement of cannabinoid CB_1 receptor desensitization in female adolescent rats following repeated Delta-tetrahydrocannabinol exposure. Br J Pharmacol 2010;161: 103–112.
16. Ruiz CM, Torrens A, Castillo E, et al. Pharmacokinetic, behavioral, and brain activity effects of Δ^9-tetrahydrocannabinol in adolescent male and female rats. Neuropsychopharmacology 2021;46:959–969; doi: 10.1038/s41386-020-00839-w
17. Torrens A, Vozella V, Huff H, et al. Comparative pharmacokinetics of Δ^9-tetrahydrocannabinol in adolescent and adult male mice. J Pharmacol Exper Ther 2020;374:151–160; doi: 10.1124/jpet.120.265892
18. Vozella V, Zibardi C, Ahmed F, et al. Fast and sensitive quantification of Δ^9-tetrahydrocannabinol and its main oxidative metabolites by liquid chromatography/tandem mass spectrometry. Cannabis Cannabinoid Res 2019;4:110–123; doi: 10.1089/can.2018.0075
19. Ruiz CM, Torrens A, Lallai V, et al. Pharmacokinetic and pharmacodynamic properties of aerosolized ("vaped") THC in adolescent male and female rats. Psychopharmacology 2021;238:3595–3605; doi: 10.1007/s00213-021-05976-8
20. Torrens A, Roy P, Lin L, et al. Comparative pharmacokinetics of Δ^9-tetrahydrocannabinol in adolescent and adult male and female rats. Cannabis Cannabinoid Res 2022;7(6):814–826; doi: 10.1089/can.2021.0205
21. U.S. Food and Drug Administration. Bioanalytical Method Validation Guidance for Industry. 2018. Available from: https://www.fda.gov/files/drugs/published/Bioanalytical-Method-Validation-Guidance-for-Industry.pdf [Last accessed: July 12, 2022].
22. Vozella V, Ahmed F, Choobchian P, et al. Pharmacokinetics, pharmacodynamics and safety studies on URB937, a peripherally restricted fatty acid amide hydrolase inhibitor, in rats. J Pharm Pharmacol 2019;71:1762–1773; doi: 10.1111/jphp.13166
23. Fotio Y, Palese F, Guaman Tipan P, et al. Inhibition of fatty acid amide hydrolase in the CNS prevents and reverses morphine tolerance in male and female mice. Br J Pharmacol 2020;177:3024–3035; doi: 10.1111/bph.15031
24. Sander LC, Pursch M, Wise SA. Shape selectivity for constrained solutes in reversed-phase liquid chromatography. Anal Chem 1999;71:4821–4830; doi: 10.1021/ac9908187
25. Kratz D, Thomas D, Gurke R. Endocannabinoids as potential biomarkers: It's all about pre-analytics. J Mass Spectrom Adv Clin Lab 2021;22:56–63; doi: 10.1016/j.jmsacl.2021.11.001
26. Zoerner AA, Gutzki FM, Batkai S, et al. Quantification of endocannabinoids in biological systems by chromatography and mass spectrometry: A comprehensive review from an analytical and biological perspective. Biochim Biophys Acta 2011;1811:706–723; doi: 10.1016/j.bbalip.2011.08.004
27. Gong Y, Li X, Kang L, et al. Simultaneous determination of endocannabinoids in murine plasma and brain substructures by surrogate-based LC–MS/MS: Application in tumor-bearing mice. J Pharm Biomed Anal 2015;111:57–63; doi: 10.1016/j.jpba.2015.03.017
28. Gurke R, Thomas D, Schreiber Y, et al. Determination of endocannabinoids and endocannabinoid-like substances in human K3EDTA plasma–LC-MS/MS method validation and pre-analytical characteristics. Talanta 2019;204:386–394; doi: 10.1016/j.talanta.2019.06.004
29. Couttas TA, Boost C, Pahlisch F, et al. Simultaneous assessment of serum levels and pharmacologic effects of cannabinoids on endocannabinoids and N-acylethanolamines by liquid chromatography–tandem mass spectrometry. Cannabis and Cannabinoid Research 2022;8(4):657–669; doi: 10.1089/can.2021.0181
30. Bobrich M, Schwarz R, Ramer R, et al. A simple LC-MS/MS method for the simultaneous quantification of endocannabinoids in biological samples. J Chromatogr B 2020;1161:e122371; doi: 10.1016/j.jchromb.2020.122371
31. Berman P, Sulimani L, Gelfand A, et al. Cannabinoidomics—An analytical approach to understand the effect of medical Cannabis treatment on the endocannabinoid metabolome. Talanta 2020;219:121336; doi: 10.1016/j.talanta.2020.121336
32. Amin MR, Ali DW. Pharmacology of medical cannabis. Adv Exp Med Biol 2019;1162:151–165; doi: 10.1007/978-3-030-21737-2_8
33. Pontis S, Ribeiro A, Sasso O, et al. Macrophage-derived lipid agonists of PPAR-α as intrinsic controllers of inflammation. Crit Rev Biochem Mol Biol 2016;51:7–14; doi: 10.3109/10409238.2015.1092944
34. Borrelli F, Romano B, Petrosino S, et al. Palmitoylethanolamide, a naturally occurring lipid, is an orally effective intestinal anti-inflammatory agent. Br J Pharmacol 2015;172:142–158; doi: 10.1111/bph.12907
35. Naderi N, Majidi M, Mousavi Z, et al. The interaction between intrathecal administration of low doses of palmitoylethanolamide and AM251 in formalin-induced pain related behavior and spinal cord IL1-β expression in rats. Neuroche Res 2012;37:778–785; doi.org/10.1007/s11064-011-0672-2
36. Laleh P, Yaser K, Alireza O. Oleoylethanolamide: A novel pharmaceutical agent in the management of obesity-an updated review. J Cell Physiol 2019;234:7893–7902; doi: 10.1002/jcp.27913
37. Igarashi M, Iwasa K, Yoshikawa K. Feeding regulation by oleoylethanolamide synthesized from dietary oleic acid. Prostaglandins Leukot Essent Fatty Acids 2021;165:102228; doi: 10.1016/j.plefa.2020.102228
38. Calignano A, La Rana G, Giuffrida A, et al. Control of pain initiation by endogenous cannabinoids. Nature 1998;394:277–281; doi: 10.1038/28393
39. LoVerme J, Russo R, La Rana G, et al. Rapid broad-spectrum analgesia through activation of peroxisome proliferator-activated receptor-alpha. J Pharmacol Exp Ther 2006;319:1051–1061; doi: 10.1124/jpet.106.111385
40. Suardíaz M, Estivill-Torrús G, Goicoechea C, et al. Analgesic properties of oleoylethanolamide (OEA) in visceral and inflammatory pain. Pain 2007; 133:99–110; doi: 10.1016/j.pain.2007.03.008
41. Russo R, LoVerme J, La Rana G, et al. Synergistic antinociception by the cannabinoid receptor agonist anandamide and the PPAR-alpha receptor agonist GW7647. Eur J Pharmacol 2007;566:117–119; doi: 10.1016/j.ejphar.2007.03.007
42. Rodríguez de Fonseca F, Navarro M, Gómez R, et al. An anorexic lipid mediator regulated by feeding. Nature 2001;414:209–212; doi: 10.1038/35102582
43. Fu J, Gaetani S, Oveisi F, et al. Oleylethanolamide regulates feeding and body weight through activation of the nuclear receptor PPAR-alpha. Nature 2003;425:90–93; doi: 10.1038/nature01921
44. Igarashi M, DiPatrizio NV, Narayanaswami V, et al. Feeding-induced oleoylethanolamide mobilization is disrupted in the gut of diet-induced obese rodents. Biochim Biophys Acta 2015;1851:1218–1226; doi: 10.1016/j.bbalip.2015.05.006
45. Balvers MG, Wortelboer HM, Witkamp RF, et al. Liquid chromatography-tandem mass spectrometry analysis of free and esterified fatty acid N-acyl ethanolamines in plasma and blood cells. Anal Biochem 2013;434:275–283; doi: 10.1016/j.ab.2012.11.008
46. Tchapla A, Heron S. Property-structure relationship of solute-stationary phase complexes occurring in molecular mechanism by penetration of eluite in bonded alkyl chains in reversed-phase liquid chromatography. J Chromatogr A 1994;684:175–188; doi: 10.1016/0021-9673(94)00596-6
47. Carr PW, Tan LC, Park JH. Revisionist look at solvophobic driving forces in reversed-phase liquid chromatography III. Comparison of the behavior of nonpolar and polar solutes. J Chromatogr A 1996;724:1–12; doi: 10.1016/0021-9673(95)00907-8
48. Sander LC, Wise SA. Shape selectivity in reversed phase liquid chromatography for separation of planar and non-planar solutes. J Chromatogr A 1993;656:335–351; doi: 10.1016/0021-9673(93)80808-L
49. Limsavarn L, Dorsey JG. Influence of stationary phase solvation on shape selectivity and retention in reversed-phase liquid chromatography. J Chromatogr A 2006;1102:143–153; doi: 10.1016/j.chroma.2005.10.035
50. Cole LA, Dorsey JG. Temperature dependence of retention in reversed-phase liquid chromatography. 1. Stationary phase conditions. Anal Chem 1992;64:317–1323; doi: 10.1021/ac00037a004
51. Dill K. The mechanism of solute retention in revered-phase liquid chromatography. J Phys Chem 1987;91:1980–1988; doi: 10.1021/j100291a060
52. Sander LC, Lippa KA, Wise SA. Order and disorder in alkyl stationary phases. Anal Bioanal Chem 2005;382:646–668; doi: 10.1007/s00216-005-3127-2

53. Röhrig W, Waibel R, Perlwitz C, et al. Identification of the oleic acid ethanolamide (OEA) isomer cis-vaccenic acid ethanolamide (VEA) as a highly abundant 18:1 fatty acid ethanolamide in blood plasma from rats and humans. Anal Bioanal Chem 2016;408:6141–6151; doi: 10.1007/s00216-016-9720-8

Cite this article as: Ahmed F, Torrens A, Mahler SV, Ferlenghi F, Huestis MA, Piomelli D (2024) A sensitive ultrahigh-performance liquid chromatography/tandem mass spectrometry method for the simultaneous analysis of phytocannabinoids and endocannabinoids in plasma and brain, *Cannabis and Cannabinoid Research* 9:1, 371–385, DOI: 10.1089/can.2022.0216.

Abbreviations Used

%RSD = percent relative standard deviation
11-COOH-THC = 11-nor-9-carboxy-Δ^9-THC
11-OH-THC = 11-hydroxy-Δ^9-THC
2-AG = 2-arachidonoyl-sn-glycerol
ANOVA = analysis of variance
CBD = cannabidiol
dMRM = dynamic multiple reaction monitoring
EDTA = ethylenediaminetetraacetic acid
EMR = Enhanced Matrix Removal
ESI = electrospray ionization
FDA = Food and Drug Administration
HOE = hemp oil extract
ISTD = [^{2}H]-containing internal standards
LLOD = lower limit of detection
LLOQ = lower limit of quantification
ND = nondetectable
OEA = oleoylethanolamide
PEA = palmitoylethanolamide
PND = postnatal day
PPAR-α = peroxisome proliferator-activated receptor-α
QC = quality control
THC = Δ^9-tetrahydrocannabinol
UHPLC-MS/MS = ultrahigh-performance liquid chromatography/tandem mass spectrometry
VEA = vaccenoylethanolamide